JOURNAL OF CATALYSIS 113, 295–306 (1988)

Solid Electrolyte Aided Study of Hydrogen Oxidation on Polycrystalline Silver

A. HILLARY AND M. STOUKIDES[1]

Department of Chemical Engineering, Tufts University, Medford, Massachusetts 02155

Received June 22, 1987; revised March 23, 1988

The silver-catalyzed hydrogen oxidation was studied in an oxygen concentration solid electrolyte cell at 280–400°C and atmospheric total pressure. The technique of solid electrolyte potentiometry (SEP) was used to monitor the thermodynamic activity of oxygen adsorbed on the catalyst surface. Oxygen was found to adsorb strongly on the surface forcing the rate to exhibit initially first-order and then negative-order kinetics. Hydrogen was very weakly adsorbed, increasing the rate almost linearly. The system did not exhibit oscillatory behavior under the experimental conditions examined, as opposed to nickel catalysts. A kinetic model that explains in a quantitative manner both kinetic and potentiometric results is presented.

INTRODUCTION

A large number of investigators have been examining recently the interaction of oxygen and hydrogen over catalytic surfaces (*1–7*). There appear to be two main reasons for that. First, there exists significant technological interest in the above reaction since H_2 has been considered as an energy "currency" in the future (*1*). Hydrogen has been proposed as one of the most desirable clean secondary energy sources which can replace fossil fuels in commercial and residential utilization. Furthermore, H_2 is catalytically more combustible at lower temperatures than any other fuel, so there is no danger of a backflash and emission of nitrogen oxides (*2*). Second, the catalytic oxidation of hydrogen has been reported to exhibit self-sustained oscillations under certain conditions (*3–7*). The metal catalysts on which such phenomena have been observed so far are platinum, palladium, and nickel (*5–7*). The appearance of oscillatory phenomena on catalytic reactions is of considerable theoretical interest and its importance has been pointed out in a number of previous studies of the subject (*8–10*).

The present paper deals with the catalytic oxidation of hydrogen over polycrystalline silver. The adsorption of O_2 on Ag has been studied in detail by numerous investigators because of its importance in the selective oxidation of ethylene to ethylene oxide (*11, 13*). Oxygen has been reported to adsorb both dissociatively and nondissociatively on Ag surfaces (*11, 12*). Significant differences exist in the reported values for heats of adsorption of oxygen (*12*), probably due to the catalyst preparation and support used. In contrast to oxygen, only a few fundamental studies have been performed regarding the adsorption of hydrogen on silver (*14–16*). It is generally accepted that hydrogen does not adsorb considerably on Ag surfaces (*16, 17*). The interaction of O_2 and H_2 over silver has also been studied previously but by rather a few investigators (*17–19*).

None of these previous works reports oscillatory phenomena for the Ag-catalyzed H_2 oxidation. In the present study, the reaction was carried out on polycrystalline silver films. The technique of solid electrolyte potentiometry (SEP) was used to monitor the thermodynamic activity of oxygen adsorbed on the catalyst surface. The above technique has been used before and shown to be very useful in cases where

---

[1] To whom correspondence should be addressed.

0021-9517/88 $3.00

transient phenomena on catalytic surfaces were monitored *in situ* (*4, 20, 21*). Particular emphasis in this study is given to comparing the present results with those obtained previously (*4, 21*) during H_2 oxidation on nickel in which the same electrochemical technique was used.

EXPERIMENTAL

The experimental apparatus as well as the basic principle of SEP has been described in detail in previous communications (*4, 21, 22*). The above technique utilizes a 8% yttria-stabilized zirconia solid electrolyte cell with one of the electrodes exposed to the reacting mixture and thus serving as a catalyst for the reaction under study. The other electrode is exposed to the ambient air and serves as the reference electrode. Assuming that atomically adsorbed oxygen is the only species to equilibrate rapidly with oxygen ions at the electrode–electrolyte interface, we can relate the open circuit voltage (EMF) of the cell with the thermodynamic activity of atomic oxygen a_O according to the equation

$$a_O = (0.21)^{1/2} \exp(2FE/RT), \qquad (1)$$

where F is the Faraday constant, R is the ideal gas constant, T is the absolute temperature, and E is the electromotive force of the cell.

The polycrystalline porous silver film preparation was the same as that described in Ref. (*23*). The silver films had an average particle size of 1 μm. On the basis of this particle size we estimated a reactive surface area of ~300 cm^2 for a 100-mg catalyst (*24*). Additional information about the experimental apparatus and procedure can be found in Refs. (*4, 24*).

RESULTS

The reaction rate and the surface oxygen activity behavior were studied at 280 to 400°C and atmospheric total pressure. The oxygen partial pressure in the reactor varied from 0.005 to 0.12 bar and that of hydrogen from 0.01 to 0.12 bar. Under the flow rates employed in this study the stabilized zirconia tube behaved as a completely mixed reactor (CSTR).

The reaction rates observed were due solely to heterogeneous effects. A "blank" reactor was used to measure the gas-phase homogeneous reaction rate under the same conditions as those employed in the catalytic study. These rates were about two orders of magnitude lower than those obtained catalytically (*24*). External and internal diffusion limitations were insignificant in the data reported below. This was confirmed by varying appropriately the volumetric flow rate and the thickness of the silver electrode film (*24*). Hence, all kinetic measurements reported below are due to intrinsic catalytic reaction.

The silver catalyst film showed a constant reactivity after an induction period of about 24 h (*24*). All data reported here were obtained after this induction period. There were no signs of deactivation for at least 5 weeks as long as the reactor temperature was kept between 250 and 400°C. All catalysts used in the present study contained 100–105 mg of silver.

The reaction rate was calculated from the appropriate mass balance for oxygen,

$$r = 2Q(X^0_{O_2} - X_{O_2}), \qquad (2)$$

where Q is the total molar flow rate, $X^0_{O_2}$, X_{O_2} are the mole fractions of oxygen in the feed and the outlet, respectively, and r is the reaction rate in moles of H_2O produced per second.

Figure 1 shows the dependence of the reaction rate and the surface oxygen activity a_O on the partial pressure of oxygen in the reactor at 280°C. The outlet partial pressure of hydrogen was maintained at either 1% (filled symbols) or 4% (open symbols). At the high H_2 concentration the rate seems to decrease with increasing oxygen until it levels off to a low value. This gradual decrease in rate with P_{O_2} is much less profound when P_{H_2} is kept at 1%. The corresponding oxygen activity seems to increase almost linearly with increasing P_{O_2}. The reaction rate

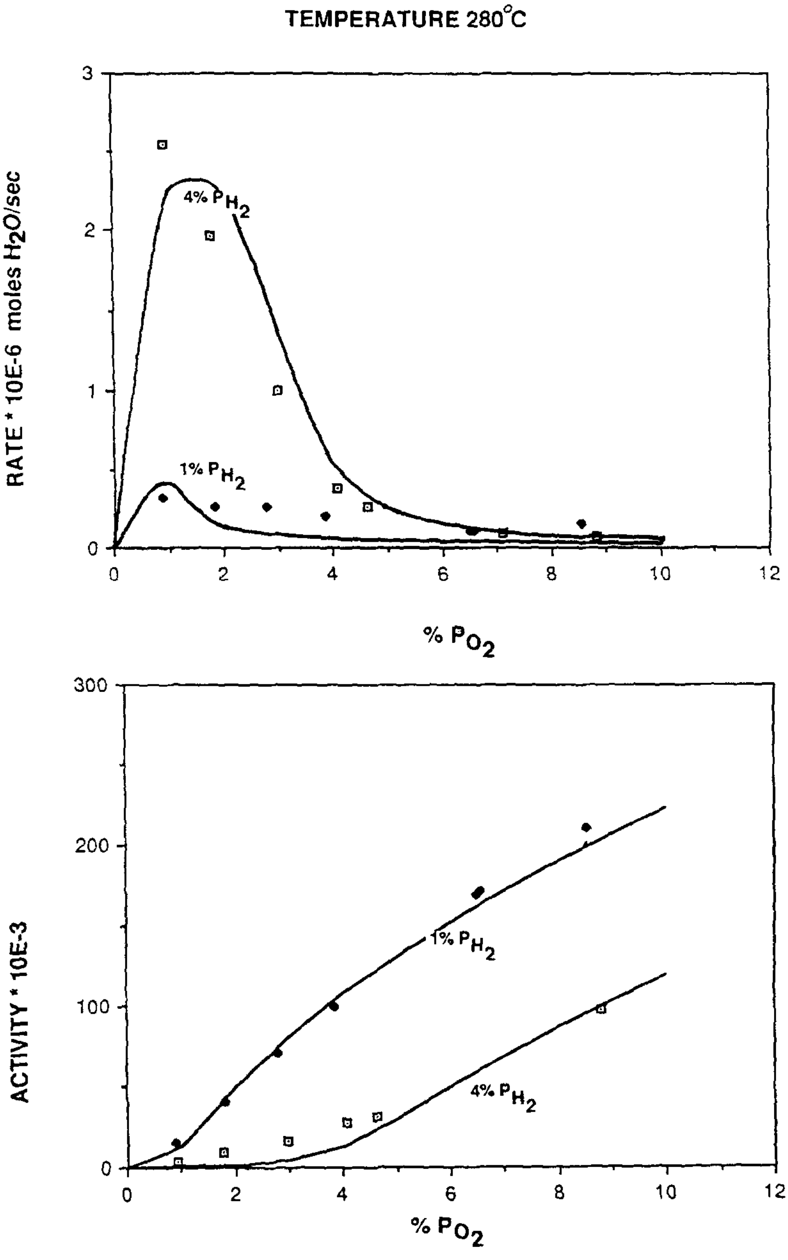

FIG. 1. Dependence of the reaction rate and the surface oxygen activity on the partial pressure of oxygen. T = 280°C; P_{H_2} = 0.01 bar (filled symbols) and 0.04 bar (open symbols). The solid lines correspond to the model predictions.

and surface oxygen activity behavior are similar at higher temperatures as shown in Figs. 2 and 3 for 320 and 360°C, respectively. It can also be seen that at very low P_{O_2} the reaction rate increases with increasing oxygen, reaches a plateau at higher P_{O_2}, and finally exhibits negative-order dependence.

Figures 4 and 5 show the effect of P_{H_2} on r and a_O at 360 and 320°C, respectively. The

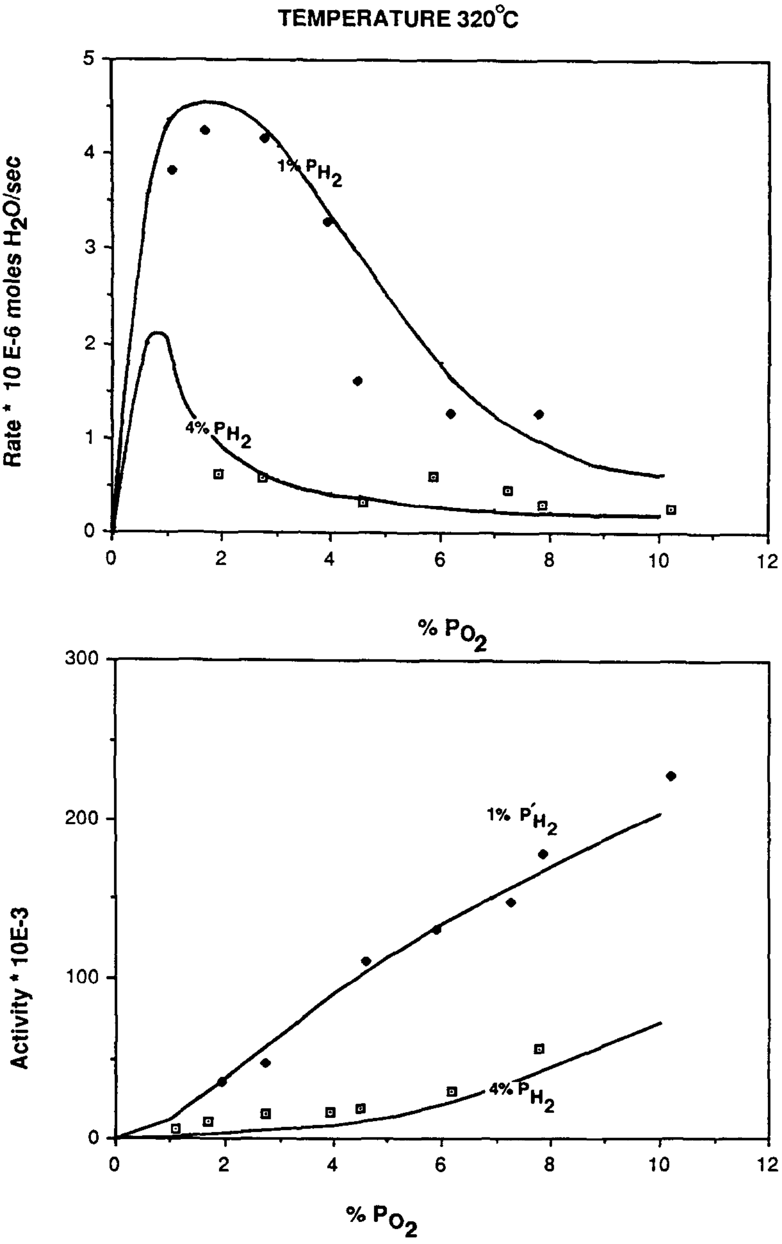

FIG. 2. Dependence of the reaction rate and the surface oxygen activity on the partial pressure of oxygen. T = 320°C; P_{H_2} = 0.01 bar (filled symbols) and 0.04 bar (open symbols). The solid lines correspond to the model predictions.

outlet partial pressure of oxygen was kept constant at either 0.01 bar (filled symbols) or 0.04 bars (open symbols). The rate increases with increasing P_{H_2} while the surface oxygen activity decreases at the same time. The behaviors are similar at all temperatures examined.

Figure 6 compares reaction rate results obtained during H_2 oxidation and Ag and Ni catalysts. The continuous lines were ob-

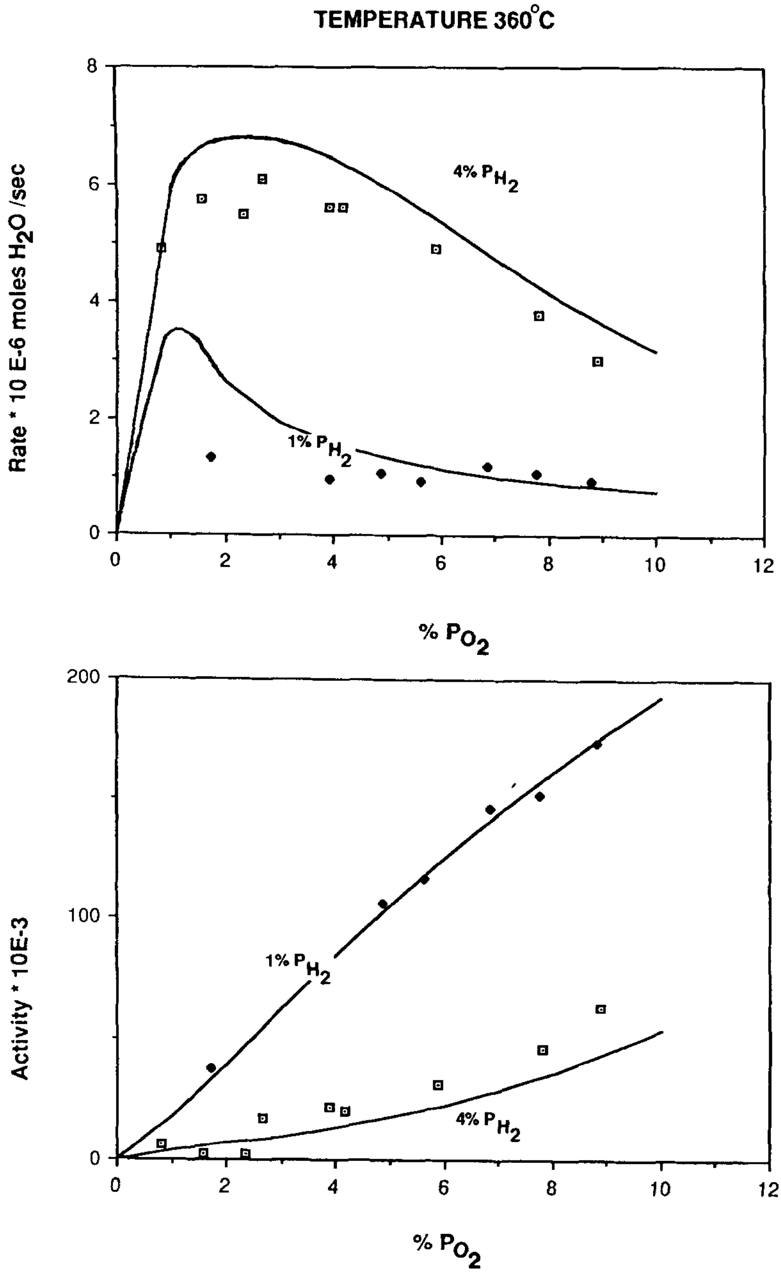

FIG. 3. Dependence of the reaction rate and the surface oxygen activity on the partial pressure of oxygen. $T = 360°C$; $P_{H_2} = 0.01$ bar (filled symbols) and 0.04 bar (open symbols). The solid lines correspond to the model prediction.

tained in a previous study over polycrystalline nickel films (*21*). The area between the two curves corresponds to the P_{H_2}/P_{O_2} and T regime within which isothermal sustained oscillations were observed on Ni. The scattered data points represent stable steady states observed on Ag catalysts in this study. It is clear that in the range of temperature and gas composition within which oscillations occur on nickel, such

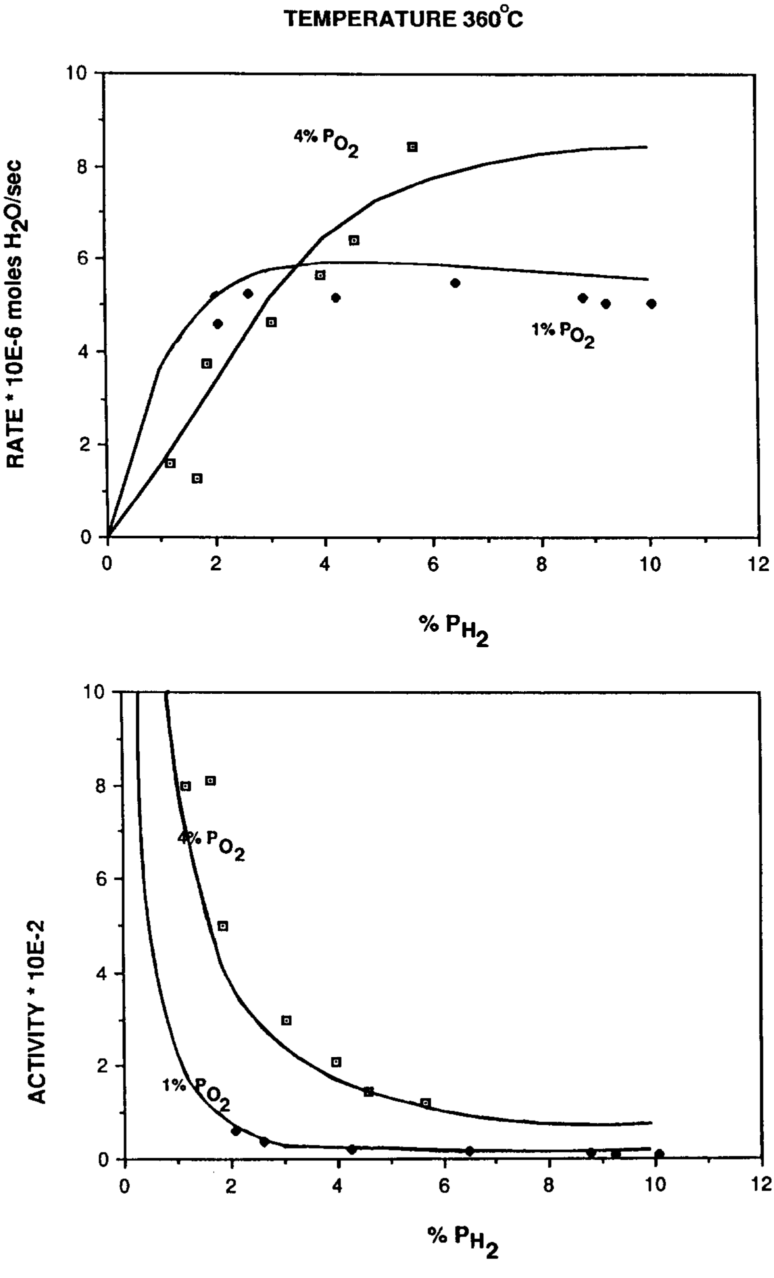

FIG. 4. Dependence of the reaction rate and the surface oxygen activity on the partial pressure of hydrogen. T = 360°C; P_{O_2} = 0.01 bar (filled symbols) and 0.04 bar (open symbols).

phenomena do not appear when using a silver catalyst. It should be pointed out that the apparatus and reactor used in the two studies were identical and the volumetric flow rates and residence times employed were comparable. In addition to the above, the catalyst loadings, the pore structures, and the average particle sizes of the nickel and silver catalyst films were very similar (*4, 21, 24*). Finally the reaction rates ob-

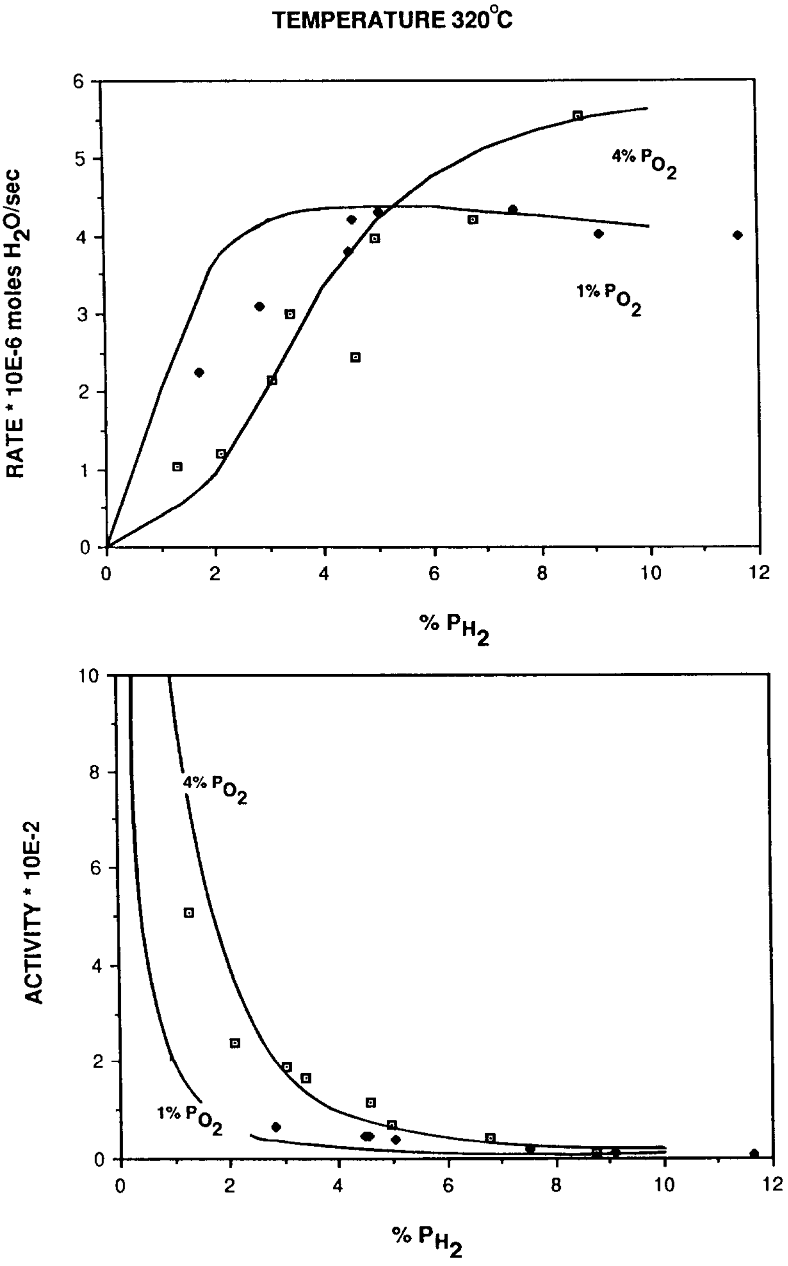

FIG. 5. Dependence of the reaction rate and the surface oxygen activity on the partial pressure of hydrogen. $T = 320°C$; $P_{O_2} = 0.01$ bar (filled symbols) and 0.04 bar (open symbols).

served on both catalysts were comparable (*21*).

At all temperatures and gas compositions examined in the present study only stable steady states were observed and there was no sign for the appearance of a periodic or aperiodic reaction rate. Stable steady states were also obtained by the surface oxygen activity that was independently measured by the SEP technique.

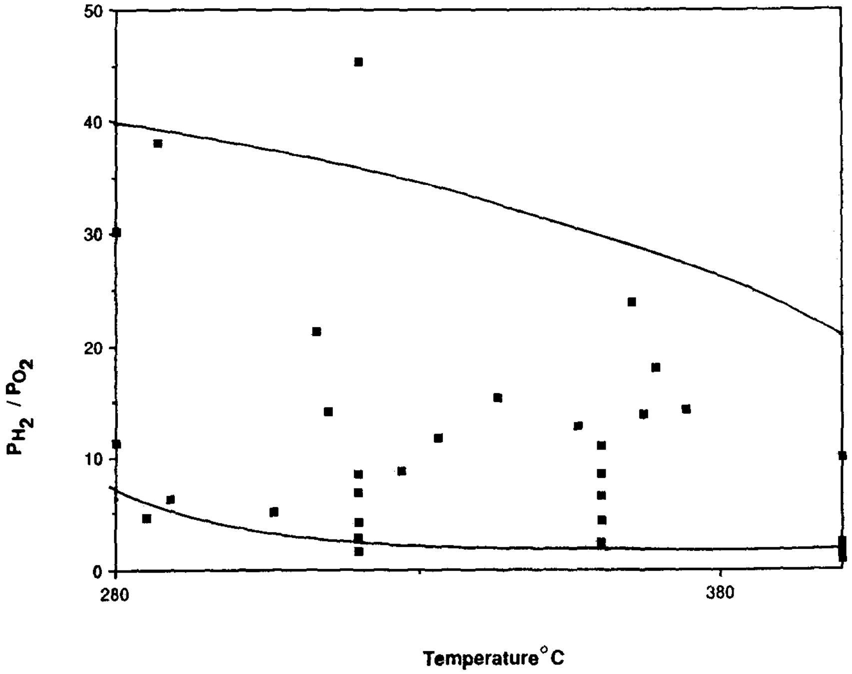

FIG. 6. Comparison of oscillatory and stable steady-state regime between nickel and silver catalysts.

DISCUSSION

The stable steady-state results presented in the previous section provided the following information:

1. The reaction rate plotted vs P_{O_2} exhibits positive- and then negative-order dependence. This implies that oxygen is strongly adsorbed on the surface or, rather, that it is adsorbed much more strongly than hydrogen.

2. The reaction rate plotted vs P_{H_2} exhibits linear dependence except for high P_{H_2} at which a weaker dependence (order between zero and one) is reached. In none of the cases, however, has a negative-order dependence on P_{H_2} been observed. This implies either negligible or weak adsorption of hydrogen on the catalyst surface.

3. If $P_{O_2}^{1/2} = a_O$, thermodynamic equilibrium is established between gaseous and adsorbed oxygen. In the study of hydrogen oxidation on Ni (*4, 21*), $P_{O_2}^{1/2}$ could exceed a_O by 2 to as much as 10 orders of magnitude. Clearly in that case the rates of adsorption of oxygen and surface reaction attained comparable values. In the present study, although a_O did deviate a little from its equilibrium value, in most cases $a_O \simeq P_{O_2}^{1/2}$ and only under certain extreme conditions (very high P_{H_2}, very low P_{O_2}, high temperatures) $P_{O_2}^{1/2}$ exceeded a_O by a factor of 5–15. Therefore in the case of H_2 oxidation on Ag the surface reaction was rate determining and only occasionally oxygen adsorption and surface reaction became comparable.

4. Rate or oxygen activity oscillations were not observed at the temperature and gas composition examined (Fig. 6). Also, the catalyst preexposure to either hydrogen or oxygen does not change the rate and a_O values obtained as opposed to the case of nickel catalysts.

The most thorough kinetic study of the Ag-catalyzed H_2 oxidation reported in the literature seems to belong to Boreskov and his co-workers (*18, 19*). According to that research group the above reaction can be represented by the model

$$O_2 \rightleftharpoons 2O_{ads} \qquad (3)$$

$$H_2 + 2O_{ads} \rightleftharpoons 2OH_{ads} \qquad (4)$$

$$H_2 + 2OH_{ads} \rightarrow 2H_2O \qquad (5)$$

where O_{ads} and OH_{ads} stand for atomically adsorbed oxygen and adsorbed hydroxyl species, respectively. In the above model the reaction of H_2 with OH_{ads} was considered the rate-determining step (*18*).

The reaction of H_2 and O_2 on Ag can be reexamined now in view of the kinetic and potentiometric information that has become available. A kinetic model proposed herein should explain not only the reaction kinetics but also the behavior of the surface oxygen activity that was independently monitored.

Although Khasin and Boreskov explained their measurements quantitatively, it was found (*24*) that the present results could not be interpreted as a whole by means of the above kinetic scheme. Furthermore step (5) implies that two adjacent adsorbed OH species collide with one gaseous molecule H_2 to form two H_2O molecules. The above step is highly unlikely to be considered elementary. In view of the present kinetic and SEP data and the existing literature concerning the O_2 and H_2 adsorption and reaction on Ag (*23, 11, 12*), the following kinetic scheme is proposed,

$$O_2 + 2S \underset{K_{11}}{\overset{K_1}{\rightleftharpoons}} 2O\text{–}S \qquad (6)$$

$$H_2 + 2S \underset{K_{22}}{\overset{K_2}{\rightleftharpoons}} 2H\text{–}S \qquad (7)$$

$$O\text{–}S + H\text{–}S \underset{K_{33}}{\overset{K_3}{\rightleftharpoons}} OH\text{–}S + S \qquad (8)$$

$$OH\text{–}S + H\text{–}S \xrightarrow{K_4} H_2O + 2S \qquad (9)$$

where S stands for a surface site and O–S, H–S, and OH–S stand for adsorbed atomic oxygen, atomic hydrogen, and hydroxyl group, respectively. The above model does not suggest that atomically adsorbed oxygen is the only oxygen species that can exist on the silver surface under these conditions. It simply considers O–S the dominant oxygen species involved in the H_2O formation.

Steps (6), (7), and (8) are assumed to be faster than step (9).

The chemical potential of adsorbed atomic oxygen can be written as

$$\mu_O(s) = A\mu^{\circ}_{O_2} + RT \ln a_O, \qquad (9a)$$

where $\mu_O(s)$, $\mu^{\circ}_{O_2}$, and a_O are the chemical potential of adsorbed atomic oxygen, the standard chemical potential of oxygen, and the activity of oxygen on the surface, respectively.

The standard state is this at which $a_O = 1$.

Similarly, we can write

$$\mu_O(s) = \tfrac{1}{2}\mu^{*}_{O_2} + RT \ln(\theta_O/\theta_S), \qquad (9b)$$

where $\mu^{*}_{O_2}$ is a new standard chemical potential and θ_O, θ_S are the fractional coverages of atomic oxygen and empty sites on the catalyst surface, respectively. Hence, the new standard state is that at which $\theta_O/\theta_S = 1$. Combining Eqs. (9a) and (9b) one gets

$$\theta_O = K_O a_O \theta_S, \qquad (10)$$

where θ_S is the coverage of empty sites and K_O is the adsorption coefficient for atomic oxygen. The above equation relates two surface properties and is valid irrespective of whether thermodynamic equilibrium exists between adsorbed and gaseous oxygen or not (*23*).

Assuming that steps (7) and (8) are in equilibrium we can write

$$\theta_H = K_H P_{H_2}^{1/2} \theta_s \qquad (11)$$

and

$$\theta_{OH} = K_{OH}\theta_O\theta_H/\theta_S, \qquad (12)$$

where K_H, K_{OH} stand for the adsorption coefficient for atomically adsorbed hydrogen and the equilibrium constant for reaction step (8), respectively. Since the slowest step is (9) we can write for the reaction rate

$$r = K_4\theta_{OH}\theta_H. \qquad (13)$$

The above rate expression becomes the one given below if we use Eqs. (10), (11), and (12):

$$r = K_O K_4 K_{OH} K_H^2 P_{H_2} a_O/(1 + K_O a_O + K_H P_{H_2}^{1/2} + K_{OH} K_O K_H P_{H_2}^{1/2} a_O)^2. \qquad (14)$$

In addition to the above equation, combining SEP and kinetic measurements, we can write a steady-state material balance for adsorbed atomic oxygen:

$$K_1 P_{O_2}^{1/2}\theta_S - K_{11}\theta_O - r = 0. \qquad (15)$$

The first term corresponds to adsorption of oxygen, the second corresponds to desorption from the surface, and the last one accounts for consumption of surface oxygen by reaction with hydrogen. Experimental justification for first-order adsorption and desorption terms has been provided previously (*23*). Using Eqs. (10), (11), and (12) and dividing by $K_1\theta_S$ all terms of Eq. (15) we can obtain

$$(P_{O_2}^{1/2} - a_O)/r = (1 + K_O a_O + K_{OH} K_H K_O P_{H_2}^{1/2} a_O + K_H P_{H_2}^{1/2})/K_O K_{11}. \qquad (16)$$

Equations (14) and (16) relate the experimentally measured r, P_{H_2}, P_{O_2}, and a_O with the temperature-dependent constants K_4, K_{OH}, K_H, K_O, and K_{11}. Previous works (*11, 12*) have provided values for K_{11} and K_O but not for K_H, K_{OH}, K_R. Using the literature values for K_{11} and K_O as first approximations, the values for K_H, K_{OH}, and K_4 were first evaluated at 320°C with the aid of the experimental data at that temperature. Then the temperature dependence of all five constants was determined by fitting the data at 400, 360, and 280°C (*24*). The final values for these constants were found to be

$$K_O = 1.3 \times 10^{-4} \exp\left(\frac{8000}{T}\right) \text{bar}^{-1/2} \qquad (17)$$

$$K_{11} = 2.61 \exp\left(-\frac{8400}{T}\right) \text{ g atoms of oxygen/s} \qquad (18)$$

$$K_H = 0.0437 \exp\left(\frac{3000}{T}\right) \text{bar}^{-1/2} \qquad (19)$$

$$K_{OH} = 0.213 \exp\left(\frac{2000}{T}\right) \qquad (20)$$

$$K_4 = 0.625 \exp\left(-\frac{5800}{T}\right) \text{ mol } H_2O/\text{s}. \qquad (21)$$

The values shown above for the kinetic and thermodynamic constants justify reasonably well the physical significance originally attributed to them. For example, the value predicted for K_H shows a weak adsorption of hydrogen (heat of adsorption only 12 kcal/mol H_2) compared to the adsorption of atomic oxygen represented by K_O. The difference in the temperature dependence of K_O and K_{11} indicates that atomic oxygen adsorption is only slightly activated (0.8 kcal/g atom of oxygen or 1.6 kcal/mol of O_2). In Figs. 1 through 5 the solid lines represent the model predictions for rate and surface oxygen activity. It can be seen that the experimental data are in good agreement with the model.

As mentioned previously, only stable steady states were observed during the oxidation on Ag in the whole range of P_{H_2}, P_{O_2}, and T examined. As shown in Fig. 6 this is in contrast to H_2 oxidation on Ni during which both surface oxygen activity and reaction rate exhibit sustained oscillations. According to previous studies (*3, 4*), the oscillatory behavior on Ni is due to periodic oxidation and reduction of the catalyst surface. Indeed SEP measurements substantiated this oxidation–reduction hypothesis as the main cause for the appearance and disappearance of oscillations (*4, 21*). Figure 7 contains thermodynamic literature

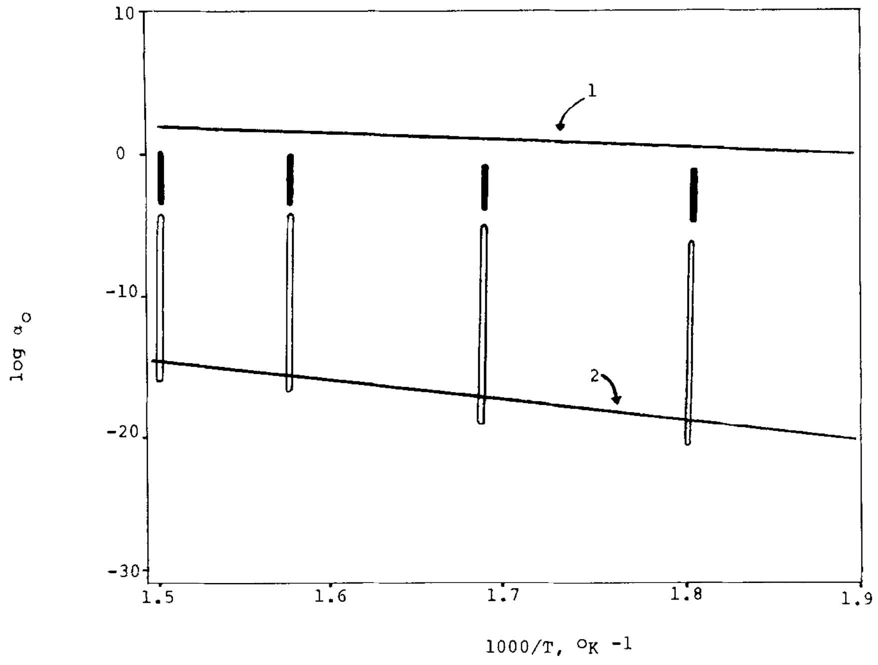

FIG. 7. Comparison of dissociation pressures of nickel oxide and silver oxide with surface oxygen activity values obtained experimentally under comparable temperature, gas composition, and residence time.

data as well as surface oxygen activity data for H_2 oxidation over Ni and Ag. The thermodynamic activity of adsorbed oxygen a_O is plotted vs the reciprocal absolute temperature. Lines 1 and 2 correspond to the stability limits of Ag_2O and NiO, respectively. Consequently, if at a given temperature the surface oxygen activity lies below line 2, formation of NiO is thermodynamically forbidden. Similarly, if a_O lies above line 1 (or 2) then formation of Ag_2O (or NiO) is thermodynamically favored. The vertical bars correspond to the range of values of a_O that were experimentally attained during the oxidation of H_2 on Ni (open bars) and on Ag (filled bars). In neither case was thermodynamic equilibrium achieved between gaseous and adsorbed oxygen. Nevertheless, this deviation from equilibrium was much more profound in the case of Ni (*21, 24*) than in the present study. In the case of Ag the values of a_O obtained were between 10^{-4} and 3×10^{-1} while for similar conditions on Ni, the a_O values were between 10^{-18} and 10^{-3}. As shown in Fig. 7 the vertical bars for Ni intersect the NiO stability curve while the bars for Ag all lie below the stability limit of Ag_2O. Physically, this means the following.

During H_2 oxidation on Ni there were cases in which the formation of NiO was favored (a_O lying above line 2) and there were cases in which formation of NiO was unfavored (a_O lying below line 2). During H_2 oxidation on Ag, formation of Ag_2O was not favored in any temperature or gas composition examined; i.e., the Ag surface was clean of silver oxide. It might have been a coincidence that oscillations were observed on Ni and not on Ag. However, the above results provide a very strong indication that the oxidation–reduction scheme, previously proposed to explain such phenomena (*3, 20*), is certainly related to the appearance and disappearance of the isothermal oscillations on nickel catalysts.

CONCLUSIONS

Kinetic and SEP measurements were combined in order to elucidate the mechanism of hydrogen oxidation on polycrystalline Ag films in a CSTR. A simple kinetic model was proposed that explains quantitatively the experimental results. According to the model, hydrogen is very weakly and oxygen is strongly adsorbed on the catalyst surface. Hydroxyl groups are formed on the surface and the rate-determining step seems to be the interaction of adsorbed OH and H species to form H_2O. The present results were compared with those obtained over Ni catalysts. Both catalysts had very similar pore and particle size characteristics. The reactors used in the two studies were identical and the temperature, gas-phase composition, and volumetric flow rates employed were the same. Isothermal oscillatory states were observed on Ni while stable steady states only were observed on Ag. It is clear that the appearance and disappearance of oscillations must be attributed to the nature of the catalyst itself rather than to any other physical phenomenon participating. A good step toward completion of this research would be to use the same apparatus and techniques to study the oxidation of hydrogen on palladium. The dissociation pressures of Ag_2O and NiO are significantly different and that of PdO lies between the above two (*3, 5, 21*). Oscillations have been observed on Pd catalysts during H_2 oxidation (*5*) and it would be very interesting to examine the behavior of the H_2–O_2 system on Pd with the aid of SEP.

ACKNOWLEDGMENT

We gratefully acknowledge the National Science Foundation for support of this work through NSF Grants CPE-8507317 and CBT-8711870.

REFERENCES

1. Norton, P. R., *in* "The Chemical Physics of Solid Surfaces and Heterogeneous Catalysis," Vol. 4. Elsevier, New York, 1982.

2. Haruta, M., Souma, Y., and Sano, H., *in* "Proceedings, 3rd World H_2 Energy Conf.," Vol. 2, p. 1135. 1980.

3. Kurtanjek, Z., Sheintuch, M., and Luss, D., *J. Catal.* **66,** 11 (1980).

4. Saranteas, C., and Stoukides, M., *J. Catal.* **93,** 417 (1985).

5. Rajagopalan, K., Sheintuch, M., and Luss, D., *Chem. Eng. Commun.* **7,** 335 (1980).

6. Belyaev, V. D., Slinko, M. M., Timoshenko, V. I., and Slinko, M. G., *Kinet. Katal.* **14,** 810 (1973).

7. Zuniga, J. E., and Luss, D., *J. Catal.* **53,** 312 (1978).

8. Sheintuch, M., and Schmitz, R., *Catal. Rev. Sci. Eng.* **15**(1), 107 (1977).

9. Slinko, M. M., and Slinko, M. G., *Kinet. Katal.* **23,** 1421 (1982).

10. Sheintuch, M., *J. Catal.* **96,** 326 (1985).

11. Kilty, R. A., and Sachtler, W. M. H., *Catal. Rev. Sci. Eng.* **10,** 1 (1974).

12. Barteau, M. A., and Madix, R. J., *in* "The Chemical Physics of Solid Surfaces and Heterogeneous Catalysis," Vol. 4. Elsevier, New York, 1982.

13. Sachtler, W. M. H., Backx, C., and Van Santen, R. A., *Catal. Rev. Sci. Eng.* **23,** 127 (1981).

14. Pritchard, J., and Tompkins, F. C., *Trans. Faraday Soc.* **56,** 540 (1960).

15. Garrido, J. A., Illas, F., Ricart, J. M., and Rubio, J., *J. Electroanal. Chem.* **196,** 387 (1985).

16. Peterson, L. G., Dannetun, H. M., and Lundstrom, I., *Phys. Rev. B.* **30**(6), 3055 (1984).

17. Ostrovskii, V. E., *Kinet. Katal.* **8**(2), 371 (1967).

18. Khasin, A. V., and Boreskov, G. K., *Kinet. Katal.* **10,** 613 (1969).

19. Gruver, V. Sh., Khasin, A. V., and Boreskov, G. K., *Kinet. Katal.* **12,** 156 (1971).

20. Vayenas, C., Georgakis, C., Michaels, J., and Tormo, J., *J. Catal.* **67,** 348 (1981).

21. Eng, D., Stoukides, M., and McNally, T., *J. Catal.* **106,** 342 (1987).

22. Wagner, C., "Advances in Catalysis" (D. D. Eley, P. W. Selwood, and P. B. Weisz, Eds.), Vol. 21, p. 323. Academic Press, San Diego.

23. Stoukides, M., and Vayenas, C., *J. Catal.* **64,** 18 (1980).

24. Hillary, A., M.S. thesis, Tufts University, 1987.